*Proceedings of the IASS 2024 Symposium*
*Redefining the Art of Structural Design*
August 26-30, 2024, Zurich, Switzerland
Philippe Block, Giulia Boller, Catherine DeWolf,
Jacqueline Pauli, Walter Kaufmann (eds.)

# Reconfigurable Inflatable Surface Structure with Tension String Patterns

Masaya TODO*, Nozomu SUDO, Tomohiro TACHI, Yoshihiro FUKUSHIMA, Kotaro IMAI

* The University of Tokyo
Hongo 7-3-1, Bunkyo-ku, Tokyo, JAPAN
todo-masaya84@g.ecc.u-tokyo.ac.jp

**Abstract**

Inflatable structures are one of the architectural structural systems that can create a variety of shapes. However, inflatable structures can ordinarily take only a single shape designed at the time of balloon manufacturing. In this study, we propose a new structural system in which various curved surface shapes can be formed from a single flat plane-shaped balloon, or air mattress, by attaching tension strings to its surface. The air mattress is constructed by controlling the distance between the membranes on both sides of the balloon through a series of parallel internal tension strings, forming a flat plate when inflated. By connecting two points on the air mattress's surface with an external restraint string shorter than the distance along the mattress's surface, the air mattress forms a curved shape when deployed. Restraint strings can be distributed over the air mattress's surface to give the air mattress extrinsic curvatures. Different patterns of strings can create a variety of curved surfaces from a single air mattress. We propose a computational design scheme for obtaining the string placement pattern from the given target surface and demonstrate the potential of this method to achieve a variety of surfaces with relatively small Gaussian curvature.

**Keywords**: structural morphology, inflatable structure, reconfigurable structure, computational design

## 1. Introduction

Inflatable structures are known for their ability to form diverse shapes [1], ease of deployment, and compactness for storage. In architecture, they have been adopted for designs like stadium domes due to their lightweight and ability to cover large spaces. Their high degree of freedom in shape and distinctive forms have led to their incorporation into many architectural structures for aesthetic reasons [2, 3]. In addition, their portability and ease of deployment also make them suitable for temporary structures, including tents [4].

A key drawback of inflatable structures, compared to other deployable structures, such as folding structures, is that they are structurally unstable if the internal membrane is not sufficiently inflated. In other words, a single inflatable structure can only maintain the stable shape predetermined during the design phase and cannot be stable in various shapes. However, there is a demand for deployable structures that can repeatedly adapt to various human activities and surrounding conditions; inflatables have not been useful for such occasions.

In this research, we propose a novel inflatable structure concept that can deform into various curved shapes by strategically placing tension strings on the surface of a flat, plate-shaped balloon – air mattress (Figure 1). A flat, plate-shaped air mattress is created by limiting the distance between the two membranes to a constant using numerous strings attached inside the balloon. Then, by connecting two points on the air mattress surface with external tension strings shorter than their geodesic distance, we can induce extrinsic curvature upon air inflation. This new inflatable structure possesses reconfigurability, where different curved shapes can be generated by varying the tension string layout pattern. This reconfigurable system consists of soft membranes and tension strings, retaining the key advantage of inflatable structures - ease of deployment and compactness for storage. Furthermore, by enabling variation in shell curvature, it can better adapt to diverse spatial requirements, site constraints, or programmatic needs.

We present a computational design approach to determine the optimal tension string pattern for deforming a flat air mattress into a desired curved shape. In recent studies of computational fabrication, the inverse problem of determining the 2D layout surfaces and constraining elements to achieve a target 3D curved surface, i.e., *programmable surfaces*, has been studied for various materials and structural forms [5, 6]. Our method follows a similar computational framework; however, the distinctive aspect of our method is that we solve the problem where not only the target 3D curved surface but also the base 2D air mattress domain is given as a constraint. This consideration allows for a single mattress to form into multiple shapes and thus allows for *reprogrammable surfaces*, which has not been considered in previous studies.

In Section 2., we first detail the proposed air mattress and tension string configuration and then describe the physical properties of this configuration. Section 3. explains the computational design scheme for tension string patterns from the target surface. In Section 4., we evaluate the potential of this approach by creating physical mock-ups.

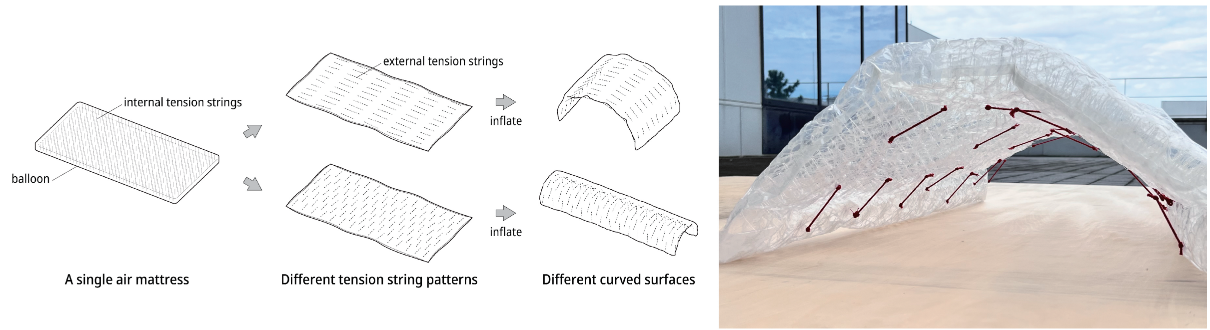


Figure 1: Left: concept of reconfigurable inflatable surface structure. Right: a mock-up of the structure.

## 2. Mechanism of reconfigurable inflatable surface structure

In this section, we first detail the configuration of the air mattress and the external tension strings (Section 2.1.) and explain the curvature formation, accompanied by experimental validation (Section 2.2.).

### 2.1. Detail of the air-mattress

To create a flat plate-shaped balloon, it is necessary to constrain the distance between the membranes on both faces of the balloon since it will otherwise inflate into a volumetric near-spherical shape. This is achieved by introducing numerous internal tension strings that connect the two membrane surfaces; such a structure, called drop stitch, is widely used for the system for obtaining flat air mattresses. In this paper, we call the resulting flat balloon composed of the membranes and internal tension strings an *air mattress*.

Grid meshes were affixed to the inner surfaces of the membranes, and plastic loops (loop pins) were installed as internal tension strings to connect corresponding grid points on the opposing faces (Figure

2). By using loop pins of uniform size and distributing them evenly, an air mattress with consistent thickness could be constructed.

To induce curvature deformations in the air mattress upon inflation, external tension strings are attached to restrain the distance between two points on the mattress surface. In our mock-ups, grid meshes were also affixed to the external surfaces, allowing strings to be tied to the mesh. Velcro stripes were adopted as external tension strings, facilitating length adjustments and pattern modifications.

In this time, we created two rectangular plane air mattress of different sizes using transparent PVC film (Large one: $2.6\,\mathrm{m} \times 1.6\,\mathrm{m}$, Small one: $830\,\mathrm{mm} \times 740\,\mathrm{mm}$, both are $70\,\mathrm{mm}$ when inflated). The grid mesh for securing the internal tension strings and external tension strings ($15\,\mathrm{mm}$ wide Velcro strips) has a grid size of $20\,\mathrm{mm}$ and was adhered to the film with tapes placed every other row and column. The loop pins were attached to the grid mesh on the inside of the film at intervals of $40\,\mathrm{mm}$ (approximately $650\,\mathrm{m}^{-2}$ density).

It is important to note that in our mock-up approach of connecting the strings to the mattress surface via the affixed grid meshes, the points where the string ends meet the mattress surface are allowed to shift within a certain range.

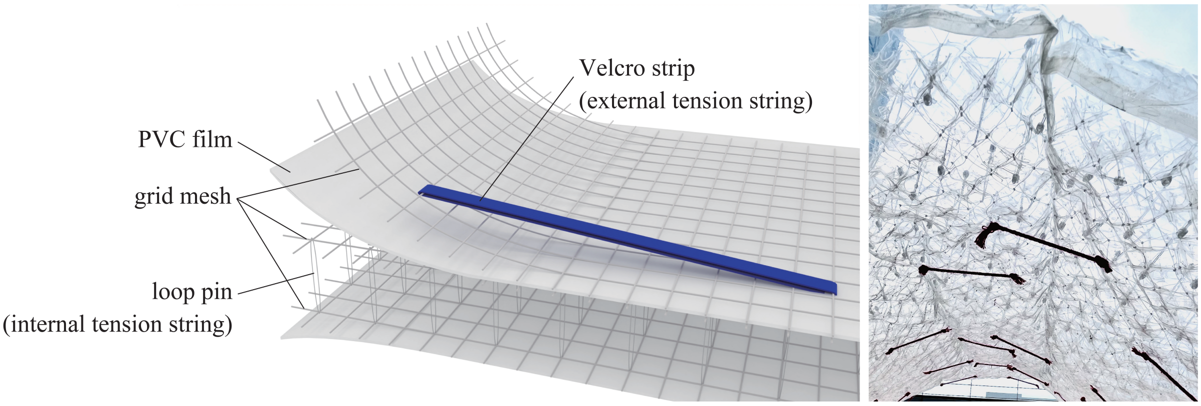


Figure 2: Left: The composition of our air mattress and external tension strings. Right: Deformation of the air mattress mock-up. The membrane is wrinkled.

### 2.2. Controlling curvature

Let $L$ be the geodesic distance between two points $A$ and $B$ on the surface of the air mattress, and $l$ be the length of the external tension string attached to connect $A$ and $B$. When $l/L$ ratio is close to 1, the air mattress remains relatively flat, whereas smaller values of $l/L$ induce greater curvature deformations.

To relate the $l/L$ ratio and the induced curvature $\kappa_1$, we conducted an experiment using the mock-up. With parallel external strings attached to the air mattress surface, inflating it results in a cylindrical shape. Keeping the string placement pattern (distance between strings and geodesic length $L = 300\,\mathrm{mm}$) fixed, we varied only the string length $l$. These cylindrical air mattress shapes were 3D scanned, and the curvature of the cross-sectional circles was measured (Figure 3).

To interpret this result, we propose a theoretical model. When an air mattress bends due to an external tension string, part of the membrane on the side attached to the string enters into the inside of the air mattress, creating a wrinkle (Figure 2). We denote the depth of this winkle as $h$. As discussed in section 2.1., in this mock-up, the ends of the tension strings are not directly attached to the membrane of the air mattress but are connected to a grid mesh attached to the membrane. Therefore, when tension occurs, the position of the string ends relative to the air mattress moves in the direction of the tension. We denote this distance of movement as $\Delta$ (Figure 4). When we set $L^* := L - 2h$ and $l^* := l + 2\Delta$, the angle of bend $\theta$ of the air mattress is related with $l^*$ and $L^*$ as

$$\sin\frac{\theta}{2} = \frac{l^*/2}{L^*/2} = \frac{l^*}{L^*}. \tag{1}$$

When we look at the membrane of the air mattress without the tension string, the length of this membrane that matches the length of the wrinkles is given by

$$(\pi - \theta)d = 2h. \tag{2}$$

Therefore, by solving the following equation derived from Equation (1) and (2), $\theta$ can be expressed in terms of $l$ and $L$.

$$\frac{l + 2\Delta}{L - (\pi - \theta)d} = \sin\frac{\theta}{2}. \tag{3}$$

The curvature measured in the experiment can be modeled as the reciprocal of the radius $R$ of the circumscribed circle of a polygon with an internal angle $\theta$ and a side length of $L^*$. Since Equation 3 cannot be solved analytically, we solve it numerically by specifying the values of the parameters [7]. In this case, we set $L = 300\,\mathrm{mm}$, $\Delta = 18\,\mathrm{mm}$, and $d = 70\,\mathrm{mm}$. Based on the calculated $\theta$, we plotted the curvature $\kappa_1 = 1/R = 2\cos\frac{\theta}{2}/L^*$ in Figure 3. It aligns well with the experimental values, in our scheme described in Section3. we calculate the string length $l$ using this theoretical value.

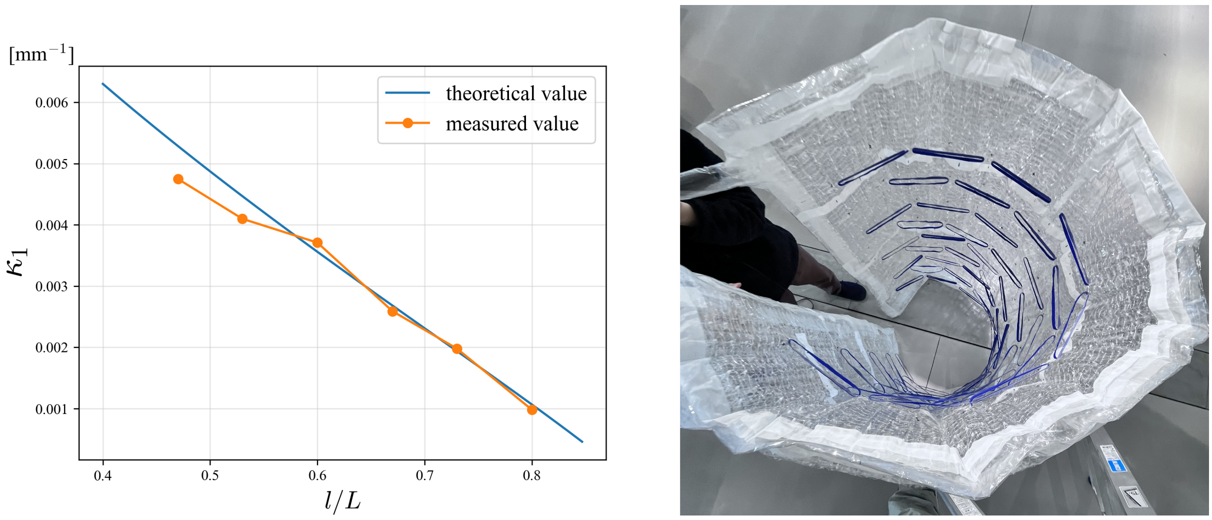


Figure 3: Left: Curvature $\kappa_1$ of the air mattress as a function of the $l/L$ ratio. Right: cylindrical shape induced by tension strings pattern.

## 3. Computational design method

In this section, we propose a computational design scheme for the inverse problem of determining the appropriate pattern of external tension strings to obtain the desired curved surface created by deforming the air mattress.

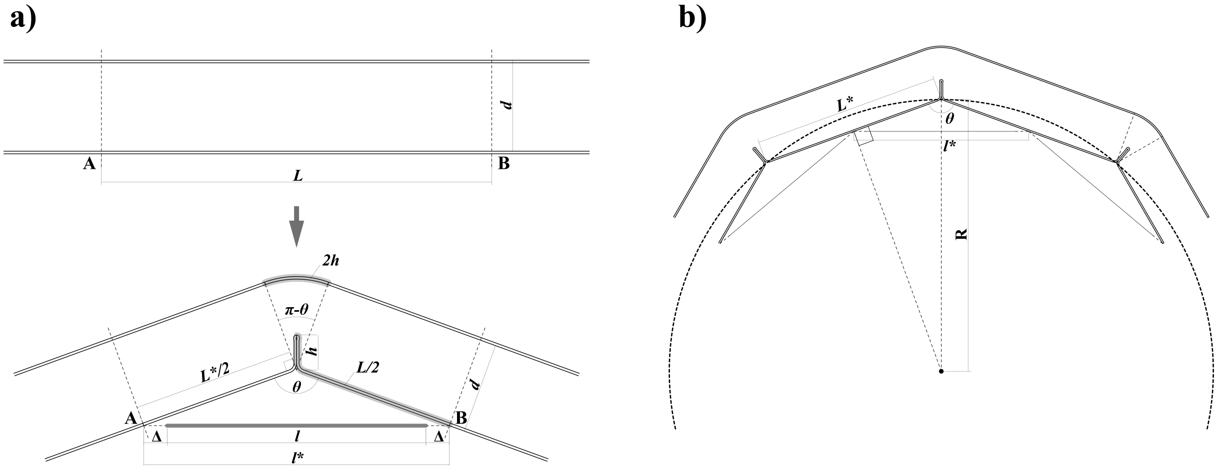


Figure 4: a) Cross-section theoretical diagram of deformation induced by a string. b) $\kappa_1$ is modeled as the reciprocal of the radius $R$ of the circumscribed circle of a polygon with an internal angle $\theta$ and a side length of $L^*$.

### 3.1. Overview

As discussed in Section 2.2., we can create single-curved surfaces by controlling the $l/L$ ratio. When the strings are attached on the top (or bottom) side, it will create the negative (or positive, resp.) curvature. Our approach is to create double curved surfaces, which have a non-zero Gaussian curvature, by overlaying the two orthogonal tension strings in the two principal curvature directions, $\mathbf{k_1}$ and $\mathbf{k_2}$, and combining their effects.

This approach can locally achieve non-zero Gaussian curvature; however, if the region with non-zero Gaussian curvature is extensive and the total angle around the perimeter of that region deviates significantly from $2\pi$, the air mattress would need to stretch significantly to conform to such a surface, which is impossible. Therefore, in our proposed inflatable shaping system, the target surface must be close to a developable surface globally, even if it is double-curved locally.

Therefore, our design framework starts by finding close-to-developable surfaces that can be made from the mattress and inversely computes the layout patterns of straps from the surface. In Section 3.2., we describe the operation of generating an approximate 3D curved surface that can be created by deforming the air mattress plane guided by a given 3D target surface. We then discuss the process of flattening the principal curvature vector field of that approximate surface onto the air mattress plane. In Section 3.3., we calculate the layout and lengths of the tension strings based on the transferred principal curvature vector field on the air mattress plane. Section 3.4. details the implementation of computer simulations used to verify the deformation of the air mattress according to the obtained tension string pattern.

### 3.2. The interactive process of generating a target surface.

To obtain design variations, we need to find surfaces that are close to developable, which can be achieved by deforming an air mattress of a fixed size. Therefore, it is necessary to first generate an approximate 3D curved surface $\widehat{\mathcal{S}} \subset \mathbb{R}^3$ that can be created by deforming the air mattress plane region $\Omega \subset \mathbb{R}^2$, guided by a given 3D target surface $\mathcal{S} \subset \mathbb{R}^3$.

To obtain an approximated $\widehat{\mathcal{S}}$ from these initial settings, a mesh $\mathcal{M} \subset \mathbb{R}^3$ is iteratively updated using the dynamic relaxation method. In this process, $\mathcal{M}$ transitions from the initial shape of $\Omega$ towards the guide $\mathcal{S}$, subject to the following constraints.

**A1** each edge of $\mathcal{M}$ keeps its length;

**A2** each vertex of $\mathcal{M}$ moves to the closest point on $\mathcal{S}$;

**A3** each vertex of $\mathcal{M}$ moves towards the average coordinates of its adjacent vertices.

To obtain an optimized $\mathcal{M}$, that is $\widehat{\mathcal{S}}$, we minimize

$$U_{\mathrm{A}} := \underbrace{\sum_{(i,j)\in E} \frac{1}{2} k_{\mathrm{A1}} \left(\epsilon_{(i,j)} - \epsilon_{0,(i,j)}\right)^2}_{U_{\mathrm{A1}}} + \underbrace{\sum_{i\in V} \frac{1}{2} k_{\mathrm{A2}} \|\mathbf{x}_i - \mathbf{x}_{i,\mathrm{closest}}\|^2}_{U_{\mathrm{A2}}} + \underbrace{\sum_{i\in V} \frac{1}{2} k_{\mathrm{A3}} \|\mathbf{x}_i - \mathbf{x}_{i,\mathrm{avg}}\|^2}_{U_{\mathrm{A3}}} . \tag{4}$$

Where:

- $U_*$ is the potential energy of constraint *;
- $k_{\mathrm{A1}}$, $k_{\mathrm{A2}}$ and $k_{\mathrm{A3}}$ are the strengths of each energy;
- $\epsilon_{(i,j)}$ is the length of edge $(i,j)$ of $\mathcal{M}$ and $\epsilon_{0,(i,j)}$ is the length of corresponding edge $(i,j)$ of $\Omega$;
- $\mathbf{x}_i$ is the position vector of vertex $i$ of $\mathcal{M}$ and $\mathbf{x}_{i,\mathrm{closest}}$ is the point on $\mathcal{S}$ that is closest to vertex $\mathbf{x}_i$;
- $\mathbf{x}_{i,\mathrm{avg}}$ is the average position vector of the neighboring vertices of $\mathbf{x}_i$;
- $E$, $V$, respectively denote the set of edges, the set of vertices in mesh $\mathcal{M}$.

To confirm whether $\widehat{\mathcal{S}}$ is constructible within our system, We verify that the ratio of edge lengths of $\widehat{\mathcal{S}}$ to the corresponding edge lengths of $\Omega$, denoted as $\sigma$, does not deviate significantly from 1, and that the maximum curvature at each point on $\widehat{\mathcal{S}}$ does not exceed the predefined upper limit. If $\widehat{\mathcal{S}}$ turns out to be an unconstructible shape, a suitable $\widehat{\mathcal{S}}$ is sought interactively by $k_{\mathrm{A1}}$, $k_{\mathrm{A2}}$ and $k_{\mathrm{A3}}$ are adjusted accordingly.

The construction of this mass-spring system and the implementation of the dynamic relaxation method are carried out using Kangaroo2 [8] on Rhinoceros and Grasshopper. Constraints A1, A2 and A3 are implemented using *EdgeLengths Goal*, *OnMesh Goal* and *Smooth Goal* in Kangaroo2.

When considering the mapping $f : \widehat{\mathcal{S}} \to \Omega$ that flattens the new target surface $\widehat{\mathcal{S}}$ obtained through the above process, for the principal direction vectors $\mathbf{k_1}$, $\mathbf{k_2}$ on $\widehat{\mathcal{S}}$, the vectors $\overline{\mathbf{k}}_\mathbf{1} = (\nabla f)^\mathsf{T}\mathbf{k_1}$, $\overline{\mathbf{k}}_\mathbf{2} = (\nabla f)^\mathsf{T}\mathbf{k_2}$ on the air mattress region $\Omega$ are computed.

### 3.3. Tension string pattern layout

Equipped with a flattened air mattress region $\Omega$, directional vectors $\overline{\mathbf{k}}_\mathbf{i} = (\nabla f)^\mathsf{T}\mathbf{k_i}$, and magnitudes $\kappa_i$, our objective is to map these to tension string parameters and compute lines on $\Omega$ representing tension strings. We use the principal curvature lines mapped on $\Omega$ and place the dashed lines along the curve.

#### *3.3.1. Pattern parameters*

Potential parameters for controlling the curvature created in the air mattress include the spacing between strings $\mu_1$, $\mu_2$ in the directions of strings and transverse direction, the geodesic distance $L$ between two points on the air mattress, and the length $l$ of the tension strings to be attached to those points. Fixing $\mu_1$, $\mu_2$, and $L$ contributes to efficient construction as it makes it easier to identify the points on the air mattress surface where the ends of the strings are attached, so we leave $l$ as the only parameter to control.

#### *3.3.2. Generating the stripe pattern*

To compute the principal curvature lines mapped on $\Omega$, we first distribute a large number of points over $\Omega$ and solve the trajectory of points when they are moved along the vector field $\overline{\mathbf{k}}_\mathbf{i}$ in positive and negative directions. The curves on $\Omega$ form the principal curvature lines. Using these curves as a guide and following the placement parameters, we sequentially position stripes of length $L$ to indicate where to attach the tension strings. To prevent the wrinkles that occur when bending from becoming continuous, we shift the stripes by a half-period relative to the dashes of the adjacent stripe, arranging them in a staggered pattern. Two string placement patterns can be obtained following $\overline{\mathbf{k_1}}$ and $\overline{\mathbf{k_2}}$.

*3.3.3. Calculating Tension String Lengths*

To calculate the length $l$ of tension strings to be attached along numerous stripes, we need to compute the representative curvature $\kappa_i$ for each stripe. First, we generate a continuous scalar field of curvature magnitude by interpolating the curvature values $\kappa_i$ defined only at the vertices of $\Omega$ [7]. Then, for each stripe, we determine the values of $\kappa_i$ at points that divide the length into $N$ equal parts from this scalar field, and we define their average value as the representative curvature value for that stripe.

### 3.4. Simulation of inflation

To confirm the validity of the tensile string placement pattern determined above, the deformation of the air mattress is simulated using Kangaroo2 on Rhinoceros/Grasshopper (Figure 5).In the initial state of the simulation, the air mattress is modeled as a closed triangular 3D mesh $\mathcal{M}' \subset \mathbb{R}^3$ with a flat rectangular outer shape, internally containing numerous strings connecting its top and bottom surfaces. Additionally, strings of length $L$ are arranged on the exterior surface of the mesh according to the designated layout pattern, with their ends fixed only to the surface of $\mathcal{M}'$. This initial state is modified using the dynamic relaxation method by providing the following constraints.

- **B1** each edge of the mesh keeps its length;
- **B2** each face of the mesh moves in the direction of its normal (outward);
- **B3** internal strings keep their length;
- **B4** each exterior string (with the initial length $L$) contracts to its calculated length $l$; and
- **B5** each vertex of the mesh moves towards the average coordinates of its adjacent vertices.

Constraints B1, B2, B3, B4, and B5 are implemented using *EdgeLengths Goal*, *Pressure Goal*, *Length(Line) Goal*, *ClampLength Goal*, and *Smooth Goal* in Kangaroo2, respectively. This simulation is equivalent to minimizing

$$U_{\mathrm{B}} := \underbrace{\sum_{(i,j)\in E'} \frac{1}{2} k_{\mathrm{B1}} \left(\epsilon_{(i,j)} - \epsilon_{0,(i,j)}\right)^2}_{U_{\mathrm{B1}}} + \underbrace{\left(-p_{\mathrm{B2}} Vol + U_{0,\mathrm{B2}}\right)}_{U_{\mathrm{B2}}} + \underbrace{\sum_{n=1}^{N} \frac{1}{2} k_{\mathrm{B3}} \left(\lambda_n - \lambda_0\right)^2}_{U_{\mathrm{B3}}} + \underbrace{\sum_{m=1}^{M} u_m}_{U_{\mathrm{B4}}} + \underbrace{\sum_{i\in V'} \frac{1}{2} k_{\mathrm{B5}} \|\mathbf{x}_i - \mathbf{x}_{i,\mathrm{avg}}\|^2}_{U_{\mathrm{B5}}} . \tag{5}$$

$$u_m := \begin{cases} \frac{1}{2} k_{\mathrm{B4}} \left(\Lambda_m - \Lambda_{0,m}\right)^2 & \text{if } \Lambda_m \geq \Lambda_{0,m}, \\ 0 & \text{otherwise.} \end{cases} \tag{6}$$

Where:

- $U_*$ is the potential energy of constraint *;
- $k_{\mathrm{B1}}$, $p_{\mathrm{B2}}$, $k_{\mathrm{B3}}$, $k_{\mathrm{B4}}$ and $k_{\mathrm{B5}}$ are the strengths of each energy;
- $\epsilon_{(i,j)}$ is the length of edge $(i, j)$ of $\mathcal{M}'$ and $\epsilon_{0,(i,j)}$ is its initial length;
- $Vol$ is the volume of $\mathcal{M}'$ and $U_{0,\mathrm{B2}}$ is the initial value of $U_{\mathrm{B2}}$;
- $N$ and $M$ respectively denote the number of internal and external tension strings;
- $\lambda_n$ is the length of the $n$-th internal tension string and $\lambda_0$ is the constant length of all internal strings;
- $\Lambda_m$ is the length of the $m$-th external tension string and $\Lambda_{0,m}$ is its target length ( $= l$);
- $\mathbf{x}_i$ is the position of vertex $i$ of $\mathcal{M}'$ and $\mathbf{x}_{i,\mathrm{avg}}$ is the average position of the its neighboring vertices;
- $E'$, $V'$, respectively denote the set of edges, the set of vertices in mesh $\mathcal{M}'$.

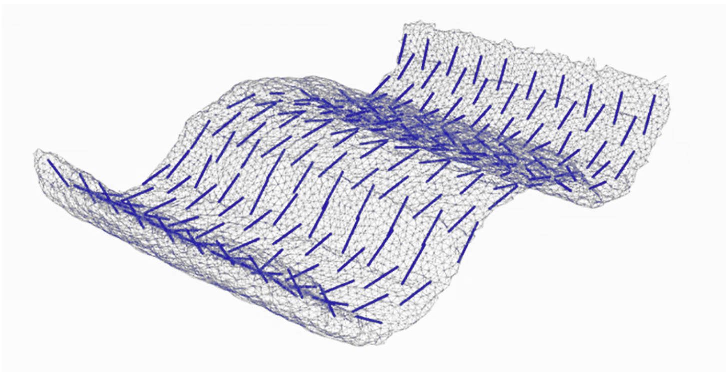

Figure 5: Simulation of inflation using a dynamic relaxation method.

## 4. Results

Figure 6 and Table 1 illustrate results produced using our method. First, we created some shapes from the small-size air mattress ($830\,\mathrm{mm} \times 740\,\mathrm{mm}$). These results illustrate that our system of curved surface formation with the air mattress and tension wires is capable of producing a variety of surface shapes, not only simple vault shapes but also surfaces with positive and negative curvatures created by attaching tension strings on both sides of the air mattress, as well as nearly developable surfaces (where $\mathbf{k_2}$ is close to zero). Furthermore, due to the air mattress's ability to contract to some extent, attaching tension strings in both directions of $\mathbf{k_1}$ and $\mathbf{k_2}$ allows for the design of double curvature surfaces with a certain degree of Gaussian curvature. It is also possible to approximate surfaces $\mathcal{S}$ with curvatures beyond this range by introducing drape-like folds to reduce the Gaussian curvature and convert into $\widehat{\mathcal{S}}$, effectively creating them from the air mattress.

We have also attempted to create more complex surfaces by applying this method to a larger air mattress ($2.6\,\mathrm{m} \times 1.6\,\mathrm{m}$). We confirmed that not only simple geometric shapes but also complex surfaces can be created from a large air mattress by defining string placement parameters based on the principal curvature of the target surface.

## 5. Conclusion

We propose a new inflatable structure composed of a flat balloon, or air mattress, whose distance between the top and bottom membranes is constrained uniformly by internal tension strings and external tension wires attached to its surface. We demonstrate that by varying the lengths of the external tension wires

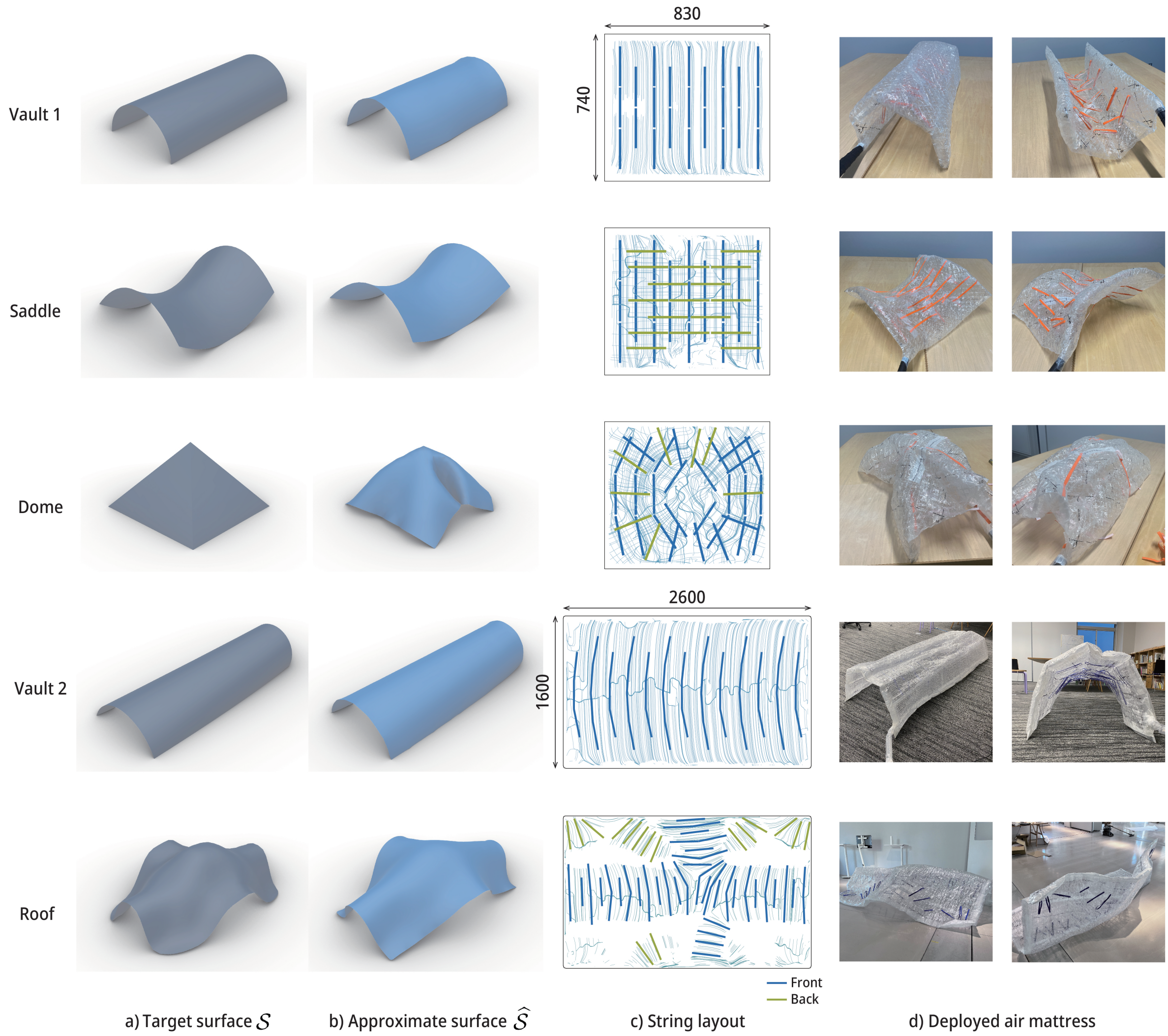


Figure 6: Five types of shapes created from two air mattresses of different sizes using our method. For each shape .

Table 1: For each shape we created in this study, we report the average and maximum value of $\sigma$ (the ratio of edge lengths of $\widehat{\mathcal{S}}$ to the corresponding edge lengths of $\Omega$) and the absolute values of curvature in the direction $\mathbf{k_1}$ and $\mathbf{k_2}$.

| **Size** | **Model** | $\sigma$ **(avg // max)** | $\lvert\kappa_1\rvert$ **(avg // max)** $[\mathrm{m}^{-1}]$ | $\lvert\kappa_2\rvert$ **(avg // max)** $[\mathrm{m}^{-1}]$ |
|---|---|---|---|---|
| small | Vault 1 | 0.9988 // 0.9661 | 3.2 // 5.2 | 0.43 // 2.0 |
| small | Saddle | 0.9933 // 0.9397 | 2.2 // 3.9 | 1.1 // 2.0 |
| small | Dome | 0.9973 // 0.9341 | 8.6 // 35 | 0.86 // 11 |
| large | Vault 2 | 0.9971 // 0.9708 | 1.8 // 3.1 | 0.15 // 1.4 |
| large | Roof | 0.9938 // 0.9421 | 2.0 // 5.8 | 0.56 // 3.3 |

relative to the geodesic distance between two points on the air mattress surface, it is possible to induce extrinsic curvature in the air mattress. We introduced a computational inverse problem-solving approach that involves attaching tension wires of lengths corresponding to the curvatures in the principal directions of the target shape, including the process of appropriately reducing the Gaussian curvature by creating folds in the target surface. Finally, by arranging external tension wires in various patterns, we showed that a single air mattress could produce a wide range of curved surface shapes, demonstrating its potential as a reconfigurable inflatable structure. Future challenges for this research include expanding the range of possible surface shapes by increasing the amount of contraction in the air mattress and developing more practical designs for the joints between the membranes and wires applicable on a larger scale.

## References

[1] M. Skouras *et al.*, "Designing inflatable structures," *ACM Trans. Graph.*, vol. 33, no. 4, 63:1–63:10, 2014. DOI: 10.1145/2601097.2601166.

[2] Y. Murata, *Expo'70 Fuji group Pavilion*. 1970.

[3] N. Howell *et al.*, "Feeling air: Exploring aesthetic and material qualities of architectural inflatables," *Adjunct Proceedings of the 2022 Nordic Human-Computer Interaction Conference*, vol. 53, pp. 1–6, 2022. DOI: 10.1145/3547522.3557781.

[4] M. Cerrahoglu and F. Maden, *A review on portable structures*, 2020.

[5] J. Panetta, F. Isvoranu, T. Chen, E. Siéfert, B. Roman, and M. Pauly, "Computational inverse design of surface-based inflatables," *ACM Transactions on Graphics*, vol. 40, no. 4, 40:1–40:14, 2021. DOI: 10.1145/3450626.3459789.

[6] D. Jourdan, M. Skouras, E. Vouga, and A. Bousseau, "Computational design of self-actuated surfaces by printing plastic ribbons on stretched fabric," *Computer Graphics Forum*, vol. 41, no. 2, pp. 493–506, 2022. DOI: https://doi.org/10.1111/cgf.14489.

[7] P. Virtanen *et al.*, "SciPy 1.0: Fundamental Algorithms for Scientific Computing in Python," *Nature Methods*, vol. 17, pp. 261–272, 2020. DOI: 10.1038/s41592-019-0686-2.

[8] R. M. Associates, *Grasshopper 3d*, https://github.com/Dan-Piker/K2Goals, 2015.